THE JOURNAL OF PHYSICAL CHEMISTRY C

Article

pubs.acs.org/JPCC

Chronoabsorptometry To Investigate Conduction-Band-Mediated Electron Transfer in Mesoporous TiO_2 Thin Films

Christophe Renault, Véronique Balland, Benoît Limoges, and Cyrille Costentin*

Laboratoire d'Electrochimie Moléculaire, UMR 7591 CNRS, Université Paris Diderot, Sorbonne Paris Cité, 15 rue Jean-Antoine de Baïf, F-75205 Paris Cedex 13, France

Supporting Information

ABSTRACT: Chronoabsorptometry response of transparent mesoporous semiconductive metal oxide film loaded with a redox-active dye is established in the framework of fast electron diffusion. It is shown that the effect of uncompensated resistance is to delay the electron accumulation in the semiconductive thin film. Consequently, this effect must be duly taken into account when interfacial charge transfer rates between the adsorbed redox species and the porous semiconductor are extracted from chronoabsorptometry responses. This is illustrated with the quantitative analysis of the chronoabsorptometry responses of a heme-based redox probe strongly adsorbed in highly ordered mesoporous TiO_2 thin films (prepared from evaporation-induced self-assembly, EISA). It is shown that the reduction of the redox probe originates from the conduction band and not from the localized traps in the bandgap. These results are in quantitative agreement with differential cyclic voltabsorptometry recently reported by us, thus showing full consistency of both methods.

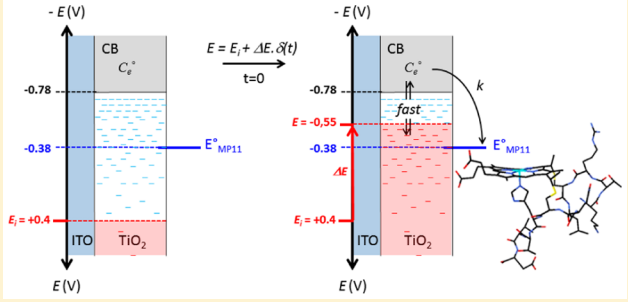

INTRODUCTION

Determination of parameters influencing charge transfer at the semiconductive metal oxide/redox dye (or redox regenerator) interface is critical to understand performances of dye-sensitized solar cells.[1,2] Such processes are indeed at work in the energy wasted recombination between injected electrons in the semiconductive metal oxide and the adsorbed oxidized dye or the electron acceptor added to the electrolyte.[3] Divergent results have appeared in the literature regarding the origin of electrons involved in the recombination step as well as the phenomena controlling its kinetics. In most cases, it was concluded that the rate constant for interfacial electron transfer between the semiconductor and the redox probe originates from localized sub-bandgap states and the dynamics being thus controlled by trap-limited electron diffusion.[4−11] However, other data were analyzed and fitted in the framework of recombination originating from the conduction band or, depending on circumstances, from traps having energies near the edge of the conduction band;[12−14] the kinetics can be described by a Gerischer-Marcus model[15,16] consistent with a reaction dynamics controlled by electron transfer rather than by electron diffusion.[17−20] It must be emphasized that different techniques have been used to investigate charge recombination from semiconductive metal oxide to a redox probe (by "redox probe" we mean any redox dye or redox couple adsorbed in a mesoporous TiO_2 film and used to probe the characteristics of the film regarding electron distribution, electron transport, and electron transfer across the film/solution interface)[4,13,21,22] as well as different kinetics models.[23−25] Moreover, different time scales have been investigated, and it must be recognized that recombination in dye-sensitized solar cells is a complex process spanning several orders of magnitude.[26] A large number of results relies on transient absorption spectroscopy measurements of oxidized dye reduction following dye excitation with a laser pulse and charge injection from the dye excited state under external applied bias.[3] With such a method, the applied potential allows for a constant concentration of electrons accumulated within the semiconductive metal oxide conduction band and intraband states (dark electrons) during the experiment. The amount of electron photoinjected remains small and is not refilled once recombined. Recombination appears to be fast, and a corresponding kinetics model has been provided leading to two limiting behaviors: slow interfacial electron transfer or dispersive electron transport.[27−29] It is on the basis of this model that experimental "stretched-exponential" decays have been interpreted as an evidence for recombination dynamics limitation based on random walk of electrons between localized sub-bandgap states.[4] Lifetimes of electrons in dye-sensitized solar cells have also been investigated by two open-circuit methods, a perturbation method, intensity-modulated photovoltage spectroscopy (IMVS),[21] and a large amplitude method, open-circuit voltage decay (OCVD).[13,22] Both methods have been shown to be equivalent, and major trends observed in experimental variation

Received: April 10, 2015
Revised: June 8, 2015
Published: June 8, 2015

DOI: 10.1021/acs.jpcc.5b03477
J. Phys. Chem. C 2015, 119, 14929−14937

of electron lifetimes under open circuit potential can be explained by a simple model only taking into account recombination from the conduction band.[7] However, a more refined model developed for OCVD was able to show that recombination can be dominated by electrons in surface traps at low open-circuit voltage.[25,22] Finally, another technique, chronoabsorptometry, relies on a large variation of the applied potential inducing electron accumulation in the semiconductive metal oxide conduction band and intraband states and enabling charge transfer to the adsorbed redox probe. In such experiments, electrons consumed by charge transfer to the adsorbed redox probe can be refilled from the underlying conductive electrode, hence leading to a faradaic component of the current. Evidence for a conduction band mediated electron transfer across nanocrystalline TiO_2 surfaces was previously obtained from chronoabsorptometry experiments;[12] however, no clear framework for electron transfer/charge transport/charge accumulation was given, thus making the data analysis and interpretation dubious. We recently showed that a simple kinetic model in conjunction with a large amplitude scanning method such as derivative cyclic voltabsorptometry (DCVA) can be useful to investigate interfacial charge transfer from a semiconductive metal oxide to a redox probe, and we provided evidence that the interfacial electron transfer from a highly ordered mesoporous TiO_2 thin film (prepared from evaporated-induced self-assembly, EISA) to heme-based redox probes is predominantly governed by the extended conduction band states of the EISA TiO_2 film.[30] The goal of the present work is to provide a simple framework to analyze chronoabsorptograms and to retrieve kinetic information with a particular emphasis on the interplay between charge accumulation and interfacial charge transfer. Analysis of experimental data obtained with microperoxidase 11 (MP-11) strongly adsorbed in highly ordered mesoporous TiO_2 film prepared from EISA will show that the proposed framework allows to retrieve the same features as obtained from DCVA. The reasons underlying the different kinetic behaviors between data gathered from potential-step transient absorption spectroscopy are discussed.

EXPERIMENTAL SECTION

Chemicals and Materials. All chemicals were provided by Sigma-Aldrich except $TiCl_4$ (Fluka). All aqueous solutions were prepared with milli-Q water (18.2 MΩ cm^{-1}) obtained from a TKA MicroPure UV purification system. Mesoporous TiO_2 thin films were prepared on commercial ITO electrodes by EISA as previously described.[31] The resulting films are characterized by a thickness of ca. 220 nm and a porosity of 0.4.[30]

Adsorption of MP-11 in Mesoporous Evaporated-Induced Self-Assembly TiO_2 Films. To perform spectroelectrochemical experiments under conditions where Soret band absorbance remains relatively stable for at least 1−2 h (i.e., negligible heme desorption), we followed the same functionalization we described previously.[30] Basically, TiO_2 films were first functionalized by soaking in a saturating solution of 50 μM MP-11 during 1 h, and the weakly adsorbed heme fraction was then removed by immersing the electrodes for 15 min in a heme-free buffer solution. The resulting modified MP-11-EISA TiO_2 electrodes were then directly used in spectroelectrochemistry.

Chronoabsorptometry. For chronoabsorptometry detection, an HR2000+ UV−visible diode-array spectrophotometer (Ocean Optics), equipped with optical fibers and a balanced deuterium tungsten source (Micropack), was coupled to an Autolab potentiostat PGSTAT 12 (EcoChemie) interfaced to a personal computer (GPES software). Both instruments were synchronized through an input trigger signal generated from the potentiostat, allowing thus to simultaneously record the change of optical UV−visible absorbance during a potential-step chronoamperometric experiment. A long pass glass color filter with a cutoff wavelength at 395 nm (GG395 filter, Ocean Optics) was installed between the light source and the sample to avoid photoexcitation of TiO_2 network during measurements. The spectroelectrochemical measurements were performed in a homemade one-compartment three-electrode cell. The TiO_2-film-coated ITO glass substrate was used as the working electrode, whereas a platinum wire and Ag/AgCl electrode in 3 M KCl were used as counter and reference electrodes, respectively (i.e., +0.21 V vs NHE at 25 °C). All potentials in the work were quoted to this reference electrode. The working electrode was prepared from a small rectangular piece of 0.8 × 3.5 cm cut from a TiO_2-film-coated ITO glass plate. A working area of 0.8 cm^2 was delimited from one extremity of the rectangular piece by depositing an insulating layer of varnish.

The three electrodes were inserted in a 1 cm path length quartz cell through a silicon cap that hermetically closes the cell. The working TiO_2-film-coated ITO electrode was positioned normal to the optical path. An additional Tygon tube (1.5 mm outer diameter) was introduced for degassing. The spectroelectrochemical cell was filled with 1.5 mL of buffer and thoroughly freed of air by bubbling with argon (at least for half an hour) prior to the experiments. During the experiments, argon was continuously flowed over the solution to maintain the anaerobic environment, and the cell was thermostated to 20 °C using a Peltier-controlled cuvette holder (Quantum Northwest). Experiments were performed in a 10 mM Hepes (pH 7.0) buffer solution, in the absence or presence of 0.1 M KCl. Integration time was fixed to 65 ms, and the experimental data results from averaging of four successive spectra leading to an effective integration time of 260 ms.

RESULTS

1. Chronoabsorptometry Response in the Framework of Fast Electron Diffusion. The reduction/oxidation rates of a redox probe adsorbed within a semiconductive film is deeply convoluted to the different modes of charge transfer/electron transport across the semiconductive nanoporous film, and we recently report that DCVA is a powerful tool for acquiring a comprehensive understanding of the dynamics of electron transfer/charge transport interlocking.[30] Despite the fundamental equivalence of all electrochemical techniques[32] it is necessary to have a closer look at expected chronoabsorptometry responses because interference of chemical capacitance charging may be different from one technique to another.

Our previous analysis with cyclic voltammetry showed that the charging current (in absence of redox probe) is not limited by electron diffusion, at least if experimental time scale is not too short, that is, $l_e = (d_f/(D_eRT/Fv)^{1/2}) \ll 1$ where d_f is the film thickness, D_e is the electron diffusion coefficient, v is the scan rate, T is the temperature, R is the gas constant, and F is the Faraday constant.[30,33] The corresponding parameter in chronoamperometry or chronoabsorptometry is $l_e = (d_f/(D_e\theta)^{1/2})$ in which θ is the time of the experiments. On the basis of the observation that absorbance decay or rise is longer than ca. 1 s (see below) in our systems, it appears that

DOI: 10.1021/acs.jpcc.5b03477
J. Phys. Chem. C 2015, 119, 14929−14937

chronoabsorptometry experiments explore the same time window as DCVA experiments previously recorded at hundreds of millivolts per second. This simple consideration of the dimensionless parameter l_e governing interference of electron diffusion in the kinetics immediately shows that absorbance decays within the second time scale in thin (sub-micrometric) films cannot provide information on electron diffusion across the semiconductive mesoporous matrix. Consequently, we restrict our analysis of chronoabsorptometry to the framework of fast electron diffusion assuming a fast delivery of a uniform electron concentration $c_e(t)$ throughout the film. Although electron injection from the underlying conductive ITO electrode to the semiconductive mesoporous matrix is assumed to be fast, establishment of the uniform electron concentration upon switching the applied potential at $t = 0$ is not instantaneous. Indeed, transport of charges requires a work from the potentiostat and a work furnished in duration equal to zero corresponds to an infinite power that the potentiostat can definitively not provide. Establishment of the uniform electron concentration within the film is thus equivalent to a capacitance charging through the uncompensated resistance of the electrochemical cell R_u and induces the existence of a capacitive current density $J_C = -(dQ/dt)$ (we adopt the convention corresponding to positive cathodic currents) where $Q = -c_e \times d_f$ is the charge injected in the semiconductive film per geometric electrode area unit. The variation of charge as a function of potential allows introducing the corresponding chemical capacitance C_{ch}. Though there is also a parallel capacitance C_S due to the underlying uncovered conductive ITO surface, its contribution can be neglected because $C_S \ll C_{ch}$.[30] As a result, $C_{ch} \approx (dQ/dE)$ (with E the potential across the semiconductive material/solution interface). As shown in Scheme 1, the potential E' imposed by the potentiostat between the working electrode (WE) and the reference electrode (RE) differs from E due to the uncompensated resistance R_u leading to $E = E' + R_uSJ$ with J the current density flowing through the cell and S the geometrical working electrode area. In chronoamperometry or chronoabsorptometry experiments the applied potential is $E' = E_i + \Delta E \times \delta(t)$, E_i being the initial potential, ΔE the potential jump, and $\delta(t)$ a step function. In most semiconductive materials, electrons may be injected in the conductive band but also in the band gap due to trap states, which is equivalent to the charging of two chemical capacitors connected in parallel (i.e., $C_{ch} = C_{cb} + C_{trap}$). Because electrons captured by trap states in typical mesoporous semiconductive films are present at a much higher density than electrons in the conduction band the total chemical capacitance can be approximated by $C_{ch} \approx C_{trap}$.[34,35] When the semiconductive film is biased negatively, the upward shift of the Fermi level (equal to $-q\Delta E$ with q the elementary charge) implies a change in the average occupancy of the trap states and of the conduction band. Assuming an ideal behavior of electrons and an energy difference between the Fermi level of the electrode (E_F) and the edge of the conduction band (E_{cb}) much larger than the thermal energy ($E_{cb} - E_F \gg k_BT$), the concentration of electrons in the conduction band when $t \to \infty$ in chronoamperometry and chronoabsorptometry can thus be expressed by[36,37]

$$c_{e,cb}(\infty) = c^0_{e,cb} \exp\left[-\frac{F}{RT}(E - E_{cb})\right]$$

with $E_{cb} = (-E_{cb}/q)$, $E = (-E_F/q)$ (in which q is the elementary charge and thus E the potential applied to the semiconductive film), and $c^0_{e,cb}$ the maximal electron concentration that can be injected at saturation in the conduction band of the semiconductive film. Trap states energies are assumed to follow an exponential distribution in the band gap leading to a density of trapped electrons when $t \to \infty$ in chronoamperometry and chronoabsorptometry experiments that varies exponentially with the Fermi level:[38]

$$c_{e,trap}(\infty) = c^0_{e,trap} \exp\left[-\frac{\alpha F}{RT}(E - E_{cb})\right]$$

where α is a dimensionless parameter that characterizes the energy distribution of the trap states below the conduction band, and $c^0_{e,trap}$ is the maximal electron concentration that can be injected in the traps.

Charging the chemical capacitance induces a capacitive contribution J_C to the current density related to C_{ch} by

$$J_C(t) = -\frac{dQ}{dt} = -C_{ch}\frac{dE}{dt}$$

with the following boundary condition when $t \to \infty$:

$$c_e(\infty) = c_{e,cb}(\infty) + c_{e,trap}(\infty) = -\frac{Q(\infty)}{Fd_f} = \frac{1}{Fd_f}\int_0^\infty J_C dt \approx c_{e,trap}(\infty)$$

Taking into account that the initial potential E_i ($t = 0$) is positive enough for the initial electron concentration to be negligible (for instance by applying a starting potential in the insulating zone of the semiconductive mesoporous film). The chemical capacitance at $t \to \infty$ is thus equivalent to

$$C_{ch} = \left(\frac{dQ}{dE}\right)_{t=\infty} = -Fd_f\left[\frac{d(c_{e,cb}(\infty) + c_{e,trap}(\infty))}{dE}\right]_{t=\infty} \approx \frac{Fd_f}{RT/F}\alpha c^0_{e,trap} \exp\left[-\frac{\alpha F}{RT}(E - E_{cb})\right]$$

which is the same apparent capacitance as in cyclic voltammetry experiments, written as[30]

$$C_{ch} = C^0_{ch} \exp\left[-\frac{\alpha F}{RT}(E - E_{cb})\right]$$

Scheme 1[a]

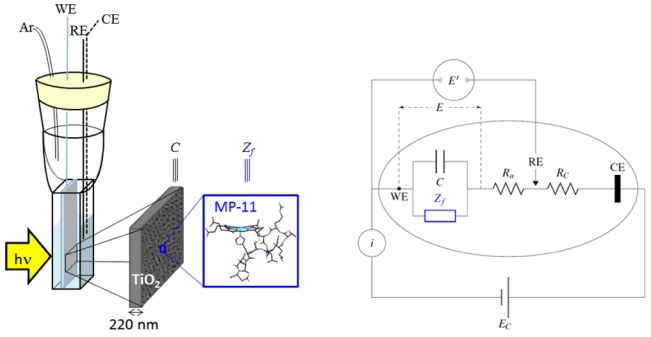

[a](left) Schematic representation of the spectroelectrochemical cell. (right) Equivalent circuit of the three-electrode electrochemical cell. WE: working electrode. RE: reference electrode. CE: counter-electrode. C: capacitance. R_u: uncompensated resistance. R_C: compensated resistance. Z_f: faradaic impedance.

DOI: 10.1021/acs.jpcc.5b03477
J. Phys. Chem. C 2015, 119, 14929−14937

with $C_{ch}^{0} = ((\alpha F^2)/RT)d_f c_{e,trap}^{0}$

In presence of a redox probe strongly adsorbed and thus nearly immobile in the mesoporous film, the total current density J is the sum of the capacitive current J_C as discussed above and of another component J_f related to the transformation of the redox probe by the electrons injected into the mesoporous matrix described as a faradaic process because electrons are transfer through the TiO_2/solution interface. Such a faradaic process is represented by the impedance Z_f in Scheme 1.

$$J = J_C + J_f$$

A decisive advantage of chronoabsorptometry as compared to chronoamperometry is to selectively record the faradaic component in the form of an integrated flux ϕ of redox molecule transformed by simply monitoring the time-course absorbance change at a given wavelength λ:

$$\phi = \frac{J_f}{nF} = \frac{1}{\Delta\varepsilon_\lambda}\frac{d\Delta A_\lambda}{dt} \text{ and } \Delta A_\lambda = \frac{\Delta\varepsilon_\lambda}{nF}\int_0^t J_f dt$$

where n is the number of electron exchanged by the redox probe, and $\Delta\varepsilon_\lambda$ is the difference between the absorption coefficient of the reduced and oxidized forms of the redox probe at the chosen wavelength. One may have the impression that the charging process, J_C, in chronoabsorptometry is discarded and so that there is no need to consider it as in the case of DCVA when compared to cyclic voltammetry. This is however true only if the charging process is fast enough compared to the faradaic one.

In accordance with the electric scheme shown in Scheme 1, we can write

$$\frac{dE}{dt} = \frac{d(E' + R_u S J)}{dt} = R_u S\frac{dJ}{dt} = -\frac{J_C}{C_{ch}}$$

If we at first consider the limiting case $J_C \gg J_f$, which corresponds to a situation where the amount of electron used to reduce the redox probe adsorbed in the mesoporous semiconductive film does not perturb significantly the charging process, then:

$$\frac{dJ_C}{dt} + \frac{J_C}{R_u S C_{ch}} \approx 0$$

Integration leads to the following implicit equation on J_C:

$$J_C \times \exp\left[\sum_{k=1}^{\infty}\frac{\left(-\frac{\alpha F}{RT}R_u S J_C\right)^k}{k \times k!}\right] = I_{C,0}\exp\left[\sum_{n=1}^{\infty}\frac{\left(-\frac{\alpha F}{RT}R_u S J_{C,0}\right)^k}{k \times k!}\right] \times \exp\left(-\frac{t}{R_u S C_{ch}^{0}\exp\left[-\frac{\alpha F}{RT}(E' - E_{cb})\right]}\right)$$

with the boundary condition:

$Q(\infty) = -\int_0^\infty J_C dt \approx -F d c_{e,trap}^{0} \times \exp[-((\alpha F)/RT)(E' - E_{cb})]$ to be used to obtain $J_{C,0}$ the initial value of J_C. Numerical calculation of this implicit equation can be made at any value of t to obtain $J_C(t)$ and $Q(t) = -\int_0^t J_C dt$. However, we make the approximation that R_u is small leading to a simple expression of the capacitive charging current:

$$J_C(t) \approx \frac{RT/F}{\alpha R_u S}\exp\left(-\frac{t}{R_u S C_{ch}^{0}\exp\left[-\frac{\alpha F}{RT}(E' - E_{cb})\right]}\right)$$

Because $J_C \approx J_{C,trap} = F d_f(dc_{e,trap}/dt)$, we then obtain

$$c_{e,trap}(t) = c_{e,trap}^{0}\exp\left[-\frac{\alpha F}{RT}(E' - E_{cb})\right] \times \left[1 - \exp\left(-\frac{t}{R_u S\frac{\alpha F d_f c_{e,trap}^{0}}{RT/F}\exp\left[-\frac{\alpha F}{RT}(E' - E_{cb})\right]}\right)\right]$$

The effect of chemical capacitance charging through the uncompensated resistance is to delay the establishment of the electron trap concentration. Although the contribution of the conduction band charging has been neglected, we can reasonably assume that the same delay affects establishment of the conduction band electron concentration leading to

$$c_{e,cb}(t) = c_{e,cb}^{0}\exp\left[-\frac{F}{RT}(E' - E_{cb})\right] \times \left[1 - \exp\left(-\frac{t}{R_u S\frac{\alpha F d_f c_{e,trap}^{0}}{RT/F}\exp\left[-\frac{\alpha F}{RT}(E' - E_{cb})\right]}\right)\right]$$

We can now derive the faradaic current in the framework of chronoamperometry corresponding to

$$J_f = -F d_f\frac{dc_O}{dt} = F d_f(k_{cb} \times c_{e,cb} + k_t \times c_{e,trap})c_O$$

where $c_O = \gamma_O/d_f$ is the volume concentration of the oxidized form of the redox probe, and γ_O is the corresponding surface concentration, while k_{cb} and k_t are the interfacial electron transfer rate constants from conduction band electrons to the redox probe and from trap electrons to the redox probe (these interfacial electron transfers were considered here irreversible on account of the standard potential of the redox probe that is far more positive than the conduction band potential, i.e. $E^{0}_{O/R} \gg E_{cb}$). It must be noted that k_t is an averaged value over the trap distribution.

Integration finally leads to

$$c_O(t) = c_O^{0}\exp\left[\begin{array}{l}\left(k_{cb} \times c_{e,cb}^{0}\exp\left[-\frac{F}{RT}(E' - E_{cb})\right]\right. \\ \left. + k_t \times c_{e,trap}^{0}\exp\left[-\frac{\alpha F}{RT}(E' - E_{cb})\right]\right) \\ \times (R_u S C_{ch})\left\{1 - \exp\left(-\frac{t}{R_u S C_{ch}}\right) - \frac{t}{R_u S C_{ch}}\right\}\end{array}\right]$$

with c_O^{0} the initial volume concentration of the oxidized form of the redox probe adsorbed in the mesoporous semiconductive film (we consider here the mesoporous film as an isotropic film where the molecules are homogeneously distributed throughout the entire volume of the film). Introducing the characteristic time constant that depends on the applied potential E':

DOI: 10.1021/acs.jpcc.5b03477
J. Phys. Chem. C 2015, 119, 14929−14937

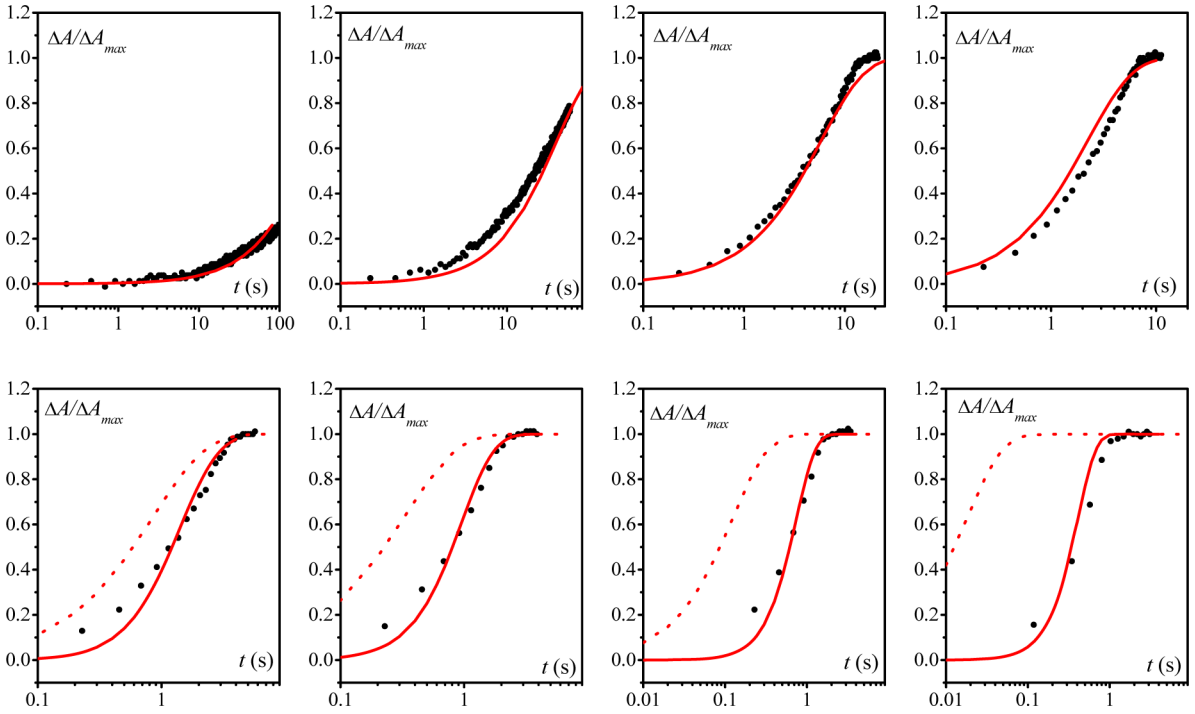

Figure 1. Time course of $(\gamma_{Fe^{II}}/\gamma^{max}_{Fe^{II}})$ changes for a MP-11-loaded EISA TiO_2 electrode ($\gamma^{max}_{Fe^{II}} = 1.1 \times 10^{-9}$ mol cm^{-2}) after stepping the potential from +0.4 V (at this potential the MP-11 is in a fully oxidized state) to (from left to right and upper to lower) −0.4, −0.45, −0.5, −0.525, −0.55, −0.575, −0.6, and −0.65 V. (- - -) Simulation with the simple exponential law eq 3. (—) Simulation with the full law expressed by eq 2.

$$\tau_C = R_u S C_{ch} = R_u S \frac{\alpha F^2 d_f c^0_{e,trap}}{RT} \exp\left[-\frac{\alpha F}{RT}(E' - E_{cb})\right]$$

the faradaic current can be written as

$$J_f(t) = J_{f,0} \exp\left[\left(\frac{\tau_C}{\tau_{cb}} + \frac{\tau_C}{\tau_{trap}}\right)\left\{1 - \exp\left(-\frac{t}{\tau_C}\right) - \frac{t}{\tau_C}\right\}\right] \quad (1)$$

showing that the charging process interferes in the faradaic process through the influence of τ_C. Here, $J_{f,0} = Fd_f(k_{cb} \times c_{e,cb} + k_t \times c_{e,trap})c^0_O$ is the initial faradaic current, while $(1/(\tau_{cb})) = k_{cb} \times c_{e,cb}{}^0 \times \exp[-(F/RT)(E' - E_{cb})]$ and $(1/\tau_{trap}) = k_t \times c_{e,trap}{}^0 \times \exp[-(\alpha F/RT)(E' - E_{cb})]$.

In the framework of chronoabsorptometry, we can write

$$\frac{\Delta A_\lambda}{\Delta A_{\lambda,\infty}} = 1 - \exp\left[\left(\frac{\tau_C}{\tau_{cb}} + \frac{\tau_C}{\tau_{trap}}\right)\left\{1 - \exp\left(-\frac{t}{\tau_C}\right) - \frac{t}{\tau_C}\right\}\right] \quad (2)$$

where $\Delta A_{\lambda,\infty}$ is the absorbance variation at the chosen wavelength when $t \to \infty$.

For chronoabsorptometric experiments where the applied potential is stepped at moderate negative values (i.e., at potential values far below the conduction band but negative to $E^0_{O/R}$) one may find experimental conditions in which the interference of the chemical capacitance charging on the transient absorbance change can be neglected ($\tau_C \ll t$). Under these conditions, eq 2 can be simplified according to a simple exponential law:

$$\frac{\Delta A_\lambda}{\Delta A_{\lambda,\infty}} = 1 - \exp\left[-\left(\frac{1}{\tau_{cb}} + \frac{1}{\tau_{trap}}\right)t\right] = 1 - \exp\left(-\frac{t}{\tau_{ET}}\right) \quad (3)$$

where the half-time is given by $t_{1/2} = \tau_{ET} \times \ln(2)$.

Conversely, if $\tau_C \gg t$ then the time-course absorbance change can be approximated by

$$\frac{\Delta A_\lambda}{\Delta A_{\lambda,\infty}} = 1 - \exp\left[-\left(\frac{1}{\tau_{cb}} + \frac{1}{\tau_{trap}}\right)\frac{t^2}{2\tau_C}\right] \quad (4)$$

where the half-time is now given by $t_{1/2} = (2\tau_C \times \tau_{ET} \times \ln 2)^{1/2}$.

2. Chronoabsorptometry of EISA TiO_2 Electrodes Loaded with MP-11. MP-11 was incorporated into the highly ordered mesoporous structure of thin films of TiO_2 coated on ITO glass plates. When the potential to sufficiently cathodic values was stepped, characteristic spectral changes associated with the electrochemical reduction of the iron center of MP-11 (from a formal oxidation state III to II) is observed (see Supporting Information, Figure S1) in line with quantitative electrochemical reduction of Fe^{III}-MP-11 within the film. The dynamics of electron/charge transport in MP-11-loaded mesoporous TiO_2 films was studied by chronoabsorptometry during which the time-course absorbance change is monitored following a potential step. The absorbance change as a function of time is monitored at a wavelength corresponding to a maxima in the difference spectra (i.e., at λ = 419 nm). From the value of $\Delta\varepsilon_\lambda = \varepsilon^{red}_\lambda - \varepsilon^{ox}_\lambda$ in TiO_2 ($\Delta\varepsilon_{419}$= 80 000 M^{-1} cm^{-1} for MP-11), the absorbance scale can be easily converted in Fe^{II} surface concentration of redox active heme (i.e., $\gamma_{Fe^{II}} = \Delta A_\lambda/\Delta\varepsilon_\lambda$ in mol/cm^2). Data are finally normalized to $\gamma_{Fe^{II}}/\gamma^{max}_{Fe^{II}} = \Delta A_\lambda/\Delta A_{\lambda,\infty}$. To investigate the influence of the applied potential on the reduction rates of MP-11 in EISA TiO_2 films, a series of chronoabsorptograms were recorded by stepping the potential from an initial value of +0.4 V to different cathodic values ranging from −0.4 to −0.65 V. Figure 1 shows the normalized time-course absorbance changes. The reduction rate of MP-11 is strongly enhanced as the potential is

DOI: 10.1021/acs.jpcc.5b03477
J. Phys. Chem. C 2015, 119, 14929−14937

increasingly negative, which is characteristic of an increase of the mesoporous TiO_2 film conductivity as the Fermi level is raised toward the conduction band. However, experimental data reveal that reduction of the adsorbed MP-11 in EISA TiO_2 films cannot be completed in less than ca. 1 s even if the potential is stepped to −0.65 V.

Previous cyclic voltammetry experiments at scan rates ranging from 5 to 100 mV/s have shown that electron transport is not rate-limiting within the time scale of the experiments,[30] that is, $l_e = ((d_f)/(D_eRT/Fv)^{1/2}) \ll 1$, thus indicating that any experiment with a characteristic time higher than 0.25 s cannot provide information on electron transport within a 220 nm thick film of TiO_2. Consequently the data gathered from chronoabsorptometry must be analyzed in the framework of fast electron diffusion, as described above, using eq 2 and taking into account that under our experimental conditions (pH = 7.0) E_{cb} = −0.78 V.[1a] Fitting experimental data with eq 2 requires two parameters, τ_c and $(1/\tau_{ET}) = (1/\tau_{cb}) + (1/\tau_{rap})$, both depending on the applied potential E'. For potentials stepped at moderate cathodic values ($E' > -0.525$ V), we assume that charging the chemical capacitance is fast enough for not interfering with the rate of interfacial electron transfer to the heme (i.e., $\tau_c \ll t$), leading to a simple exponential law for absorbance change as described by eq 3. It is thus possible to fit the data at each potential ($E' = -0.4$ to −0.525 V) with a single parameter, τ_{ET}. Figure 1 shows that data can be satisfactorily fitted with $(1/\tau_{ET}) = k_{cb}c_{e,cb}^{0} \times \exp[-((F/RT)(E' - E_{cb}))]$, taking $k_{cb}c_{e,cb}^{0} = 8 \times 10^3$ s^{-1} the exact same value as the one obtained previously from DCVA experiments under the same experimental conditions and with negligible contribution of electron transfer from electrons in trap states.[30]

As the applied potential is stepped to more negative potentials (E'= −0.55 to −0.65 V), variation of the absorbance predicted from the simple exponential eq 3 (i.e., taking $k_{cb}c_{e,cb}^{0} = 8 \times 10^3$ s^{-1}) is much too fast as compared to the experimental data (dashed lines in Figure 1). This discrepancy cannot be ascribed to contribution of electron transfer from electrons in trap states because, α being smaller than unity, contribution of electron transfer from electrons in trap states relative to contribution from the conduction band is expected to be less important as the potential is more negative. We thus conclude that the observed deviation from the simplified law is due to interference of chemical capacitance charging, which effect is to delay the establishment of electron concentration in TiO_2 film, thus decreasing the apparent electron transfer process. Data must thus be fitted with the full kinetics law corresponding to eq 2 using τ_c as fitting parameter and the same value of $(1/\tau_{ET}) = k_{cb}c_{e,cb}^{0} \exp[-((F/RT)(E' - E_{cb}))]$, taking $k_{cb}c_{e,cb}^{0} = 8 \times 10^3$ s^{-1}. Values of τ_c are reported in Figure 2. As expected, log τ_C is a linear increasing function as the applied potential E' is increasingly negative. From the slope of 7.6 V^{-1} in Figure 2 it can be inferred a value of α = 0.45, slightly higher than the value previously estimated (i.e., 0.32) from the TiO_2 charging current in cyclic voltammetry.[30] However, this value is much smaller than unity, thus clearly demonstrating that the charging current is dominated by trap filling as assumed in our model description. Taking R_u = 1500 Ω, S = 0.8 cm^2, E_{cb} = −0.78 V, we obtain $c_{e,trap}^{0}$ = 1 M. This corresponds to a density of electron in traps of ca. 1×10^{21} per cm^3 taking into account the void volume of the film (0.4), a value that appears higher than the values previously reported for mesoscopic films of sintered TiO_2 nanoparticles (a few 1×10^{19} per cm^3).[9,34] On the basis of the numerous assumptions made, we may consider our result as a reasonable value.

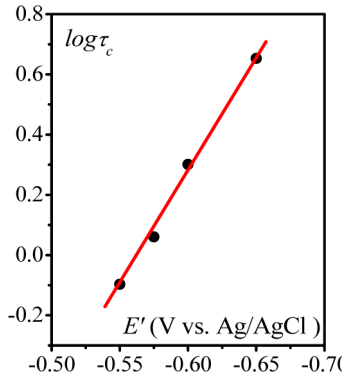

Figure 2. Variation of τ_c with the applied potential E'. (—) Linear fit.

To further confirm the influence of the capacitance charging through the cell resistance on the experimental data, chronoabsorptometry experiments were repeated in the presence of 0.1 M KCl using the same MP-11-loaded EISA TiO_2 electrode and by stepping the potential to increasingly cathodic values. It is shown in Figure 3 that when the potential is stepped from +0.4 to −0.525 V there is insignificant difference between the data in presence or in absence of KCl, and both set of data can be reasonably fitted with eq 3, which thus corresponds to the simple exponential law with no influence of τ_C. When the potential is stepped from +0.4 to −0.55 V or more negative potential, there is a noticeable difference in the data gathered with and without KCl. In presence of KCl the absorption variation is faster. When the applied potential is −0.55 V, the trace obtained in the presence of KCl can still be fitted by a simple exponential law, indicating no influence of capacitance charging, whereas in the absence of KCl the capacitance charging through the resistance delays the absorbance growth, showing thus that, as expected, the uncompensated resistance R_u is smaller in the presence of a higher ionic strength. When the potential is stepped to more negative potentials (−0.6 and −0.65 V) the data in the presence of KCl also deviate from the simple exponential law. Fitting the data with the full kinetics law (eq 2) allows to estimate the remaining uncompensated resistance in the presence of 0.1 M KCl as being of the order of 200 Ω.

DISCUSSION

In this paper we have provided a framework to analyze chronoamperometry and chronoabsorptometry experiments in semiconductive mesoporous films with adsorbed redox probes in the framework of fast electron diffusion. Electron diffusion could interfere in the dynamics of such experiments only if $(d_f^2/\sqrt{D_e}) \geq \tau$, where τ is the characteristic time of competitive processes occurring between capacitance charging and electron transfer from the semiconductive film to the redox probe, leading thus to two limiting half-time decays (or rise), that is, τ_{ET} ln 2 and $(2\tau_{ET}\tau_C \text{ ln } 2)^{1/2}$. These limiting half-time decays (or rise) are increasing function of the negatively applied potential making it, in principle, possible to fulfill the condition for electron transport interference, but the current time resolution of the chronoabsorptometry experiments (ca. 0.2 s) is a limitation. In the case of the thin mesoporous TiO_2 films (220 nm thick) investigated here this condition is not met before reaching the experimental time resolution limit. Much

DOI: 10.1021/acs.jpcc.5b03477
J. Phys. Chem. C 2015, 119, 14929−14937

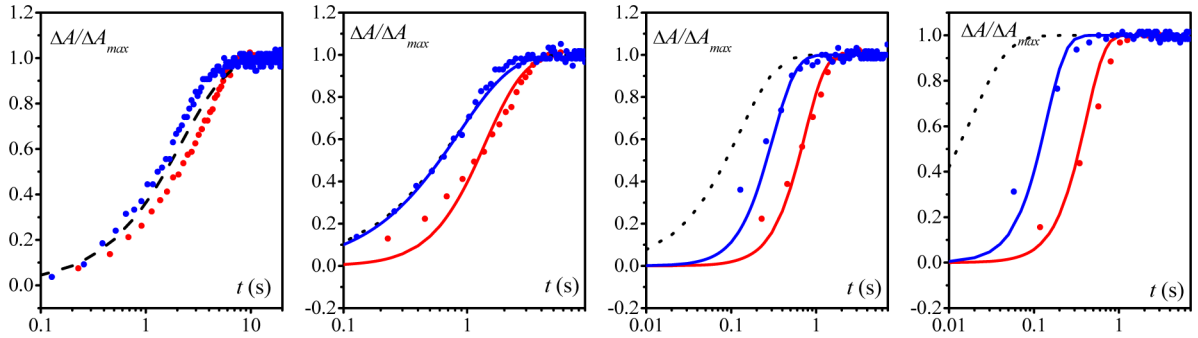

Figure 3. Time course of $(\gamma_{Fe^{II}}/\gamma_{Fe^{II}}^{max})$ changes for a MP11-loaded EISA TiO_2 electrode after stepping the potential from +0.4 V to (from left to right) −0.525, −0.55, −0.6, and −0.65 V in absence (red ●, same data as in Figure 2) or presence (blue ●) of 0.1 M KCl. (dashed black line) Simulation with the simple law (eq 3). (full lines) Simulation with the full law (eq 2).

thicker films would be required to get information on electron diffusion dynamics.

The present analysis shows that retrieving information on the electron transfer corresponding to redox probe reduction by electron injected in the semiconductive matrix requires taking into account the chemical capacitance charging through the uncompensated resistance of the electrochemical cell. We have shown that the effect of capacitance charging is to delay the establishment of electron concentration in the semiconductive matrix. This leads to a "stretched" exponential decay (or rise) as exemplified in Figure 4. Such a stretched exponential decay (or

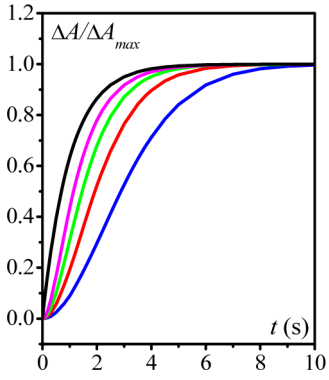

Figure 4. Simulated time-course changes of $(\Delta A/\Delta A_{max})$ using eq 2. The simulations were achieved using a constant value of τ_{ET} = 1 s and the following different values of τ_C: (blue) 5 s, (red) 2 s, (green) 1 s, (magenta) 0.5 s, and (black) $\tau_C \rightarrow 0$ (the latter corresponds thus to eq 3).

rise) may seem reminiscent of stretched exponential decays observed for charge recombination following dye excitation studied by transient absorption spectroscopy and exhibiting applied bias dependence.[4,27] However, this corresponds to a different situation. Transient absorption spectroscopy studies of recombination reactions between electrons injected in nanostructured TiO_2 films and adsorbed dyes lead to decays in the sub-microsecond to millisecond regime, depending on the applied bias,[4] which is much faster than the time decays observed here in chronoabsorptometry experiments. Consequently transient absorption spectroscopy data have been interpreted in the framework of kinetics dominated by a charge transport controlled by the release of electrons from trap states, which is in line with the observation of a power-law corresponding to the dispersive nature of such kinetics.[27] Investigation of electron transport dynamics was made possible in those cases because (i) there is a priori no limitation by chemical capacitance charging through a resistance inherent to chronoabsorptometry and (ii) time resolution of transient absorption spectroscopy is much smaller. One may however wonder why electron transfer from semiconductive matrix to redox probe is much faster in most reported transient absorption spectroscopy experiments than in chronoabsorptometry. It must be emphasized that there is a large body of data on $TiO_2(e^-)$−redox probe charge transfer in the literature leading to conflicting conclusions: some studies conclude that kinetics is controlled by electron transport, while other studies concluded that electron transfer kinetics is rate-determining and is either the inverted Marcus region or near the top of the Marcus curve.[3,17,39] Undoubtedly, these differences arise from details of the preparation of the TiO_2 thin films, surface chemistry such as $TiCl_4$ pretreatments, and species present in the electrolyte as well as molecular structure of the redox probe inducing variable physical separation from the semiconductive surface.[40] We propose that the observed differences between transient absorption spectroscopy of charge recombination and chronoabsorptometric experiments may also arise from differences in charge injection processes. In the first case electron injection occurs from a dye excited state leading to electron trapping in intraband surface states, thus giving rise to a fast recombination dominated by trapping and detrapping of electrons from surface trap states.[41] In the second case, electrons are injected in the semiconductive matrix from the underlying conductive electrode thus filling conduction band states and intraband states, which may be different from surface states. Consequently, electron transfer to the adsorbed redox probe from trap states deeply buried inside the semiconductive matrix are too slow, and electron transfer only occurs from the conduction band but again at a slower rate than from surface trap states. It is indeed remarkable that analysis of chronoabsorptometric data on MP-11 adsorbed in EISA TiO_2 thin films leads to the same conclusion as our previous analysis of the very same system by DCVA.[30] The reduction of the redox probe originates from the conduction band and not from the localized traps in the bandgap, and the same reduction rate constant was derived independently using both techniques, thus showing full consistency of the analysis.

Comparison of our results with recombination of photogenerated electrons in dye-sensitized solar cells investigated by OCVD may seem pertinent because both techniques (OCVD and chronoabsorptometry) are dark large amplitude measurements. There are however fundamental differences between both techniques. In chronoabsorptometry, electron transfer

DOI: 10.1021/acs.jpcc.5b03477
J. Phys. Chem. C 2015, 119, 14929−14937

from the semiconductive matrix to the redox probe is investigated, while electron concentration in the semiconductive matrix is maintained constant through fast refill of electrons thanks to the applied bias. In OCVD, it is the opposite situation because the measurements basically correspond to electron dump from the semiconductive matrix. Consequently, even if electron transfer originates from conduction band, intraband traps will be emptied through a trapping−detrapping process, and the measured lifetime will be sensitive to a trap distribution. This is not the case in chronoabsorptometry except at short times where concentrations of electron in the semiconductive matrix are not yet established, and we have seen that the measurement is then perturbed by trap filling even though recombination only occurs from the conduction band. It must be mentioned that OCVD experiments showed that electron lifetime is dominated by surface traps at low open-circuit voltage. No such behavior was observed in our chronoabsorptometry experiments maybe because we did not investigate positive enough potentials. Finally, we would say that analysis of electron recombination through chronoabsorptometry is maybe more relevant than OCVD regarding dye-sensitized solar cells because it allows an analysis of the recombination at steady-state concentration of electrons in the semiconductive matrix as would be the case in dye-sensitized solar cells under continuous irradiation.

CONCLUSION

In this work, chronoabsorptometry response of transparent mesoporous semiconductive metal oxide film loaded with a redox-active dye have been established in the framework of fast electron diffusion. It is shown that the effect of uncompensated resistance is to delay the electron accumulation in the semiconductive thin film leading to a possible stretched exponential decay (or rise) of the redox dye absorbance. Quantitative analysis of the chronoabsorptometry responses of a heme-based redox probe strongly adsorbed in highly ordered mesoporous TiO_2 thin films shows that the reduction of the heme originates from the conduction band and not from the localized traps in the bandgap. These results are in quantitative agreement with differential cyclic voltabsorptometry results recently reported thus showing full consistency of both methods.

ASSOCIATED CONTENT

Supporting Information

Characteristic spectral changes associated with the electrochemical reduction of the iron center of MP-11. The Supporting Information is available free of charge on the ACS Publications website at DOI: 10.1021/acs.jpcc.5b03477.

AUTHOR INFORMATION

Corresponding Author

*E-mail: cyrille.costentin@univ-paris-diderot.fr. Phone: +33157278796.

Notes

The authors declare no competing financial interest.

ACKNOWLEDGMENTS

This work was supported by Agence National pour la Recherche (ANR 3D-BIOELEC).

REFERENCES

(1) Hagfeldt, A.; Grätzel, M. Light-Induced Redox Reactions in Nanocrystalline Systems. *Chem. Rev.* **1995**, *95*, 49−68.
(2) Grätzel, M. Photoelectrochemical Cells. *Nature* **2001**, *414*, 338−344.
(3) Ardo, S.; Meyer, G. J. Photodriven Heterogeneous Charge Transfer with Transition-Metal Compounds Anchored to TiO_2 Semiconductor Surfaces. *Chem. Soc. Rev.* **2009**, *38*, 115−164.
(4) Haque, S. A.; Tachibana, Y.; Klug, D. R.; Durrant, J. R. Charge Recombination Kinetics in Dye-Sensitized Nanocrystalline Titanium Dioxide Films under Externally Applied Bias. *J. Phys. Chem. B* **1998**, *102*, 1745−1749.
(5) Haque, S. A.; Tachibana, Y.; Willis, R. L.; Moser, J. E.; Grätzel, M.; Klug, D. R.; Durrant, J. R. Parameters Influencing Charge Recombination Kinetics in Dye-Sensitized Nanocrystalline Titanium Dioxide Films. *J. Phys. Chem. B* **2000**, *104*, 538−547.
(6) Nelson, J.; Haque, S. A.; Klug, D. R.; Durrant, J. R. Trap-Limited Recombination in Dye-Sensitized Nanocrystalline Metal Oxide Electrodes. *Phys. Rev. B* **2001**, *63*, 205321.
(7) Willis, R. L.; Olson, C.; O'Regan, B.; Lutz, T.; Nelson, J.; Durrant, J. R. Electron Dynamics in Nanocrystalline ZnO and TiO_2 Films Probed by Potential Step Chronoamperometry and Transient Absorption Spectroscopy. *J. Phys. Chem. B* **2002**, *106*, 7605−7613.
(8) Green, A. N. M.; Palomares, E.; Haque, S. A.; Kroon, J. M.; Durrant, J. R. Charge Transport versus Recombination in Dye-Sensitized Solar Cells Employing Nanocrystalline TiO_2 and SnO_2 Films. *J. Phys. Chem. B* **2005**, *109*, 12525−12533.
(9) van de Lagemaat, J.; Franck, A. J. Effect of the Surface-State Distribution on Electron Transport in Dye-Sensitized TiO_2 Solar Cells: Nonlinear Electron-Transport Kinetics. *J. Phys. Chem. B* **2000**, *104*, 4292−4294.
(10) Zhu, K.; Kopidakis, N.; Neale, N. R.; van de Lagemaat, J.; Franck, A. J. Influence of Surface Area on Charge Transport and Recombination in Dye-Sensitized TiO_2 Solar Cells. *J. Phys. Chem. B* **2006**, *110*, 25174−25180.
(11) Bisquert, J.; Zaban, A. The Trap-Limited Diffusivity of Electrons in Nanoporous Semiconductor Networks Permeated with a Conductive Phase. *Appl. Phys. A: Mater. Sci. Process.* **2003**, *77*, 507−514.
(12) Staniszewski, A.; Morris, A. J.; Ito, T.; Meyer, G. J. Conduction Band Mediated Electron Transfer Across Nanocrystalline TiO_2 Surfaces. *J. Phys. Chem. B* **2007**, *111*, 6822−6828.
(13) Zaban, A.; Greenshtein, M.; Bisquert, J. Determination of the Electron Lifetime in Nanocrystalline Dye Solar Cells by Open-Circuit Voltage Decay Measurements. *ChemPhysChem* **2003**, *4*, 859−864.
(14) Gaal, D. A.; Hupp, J. T. Thermally Activated, Inverted Interfacial Electron Transfer Kinetics: High Driving Force Reactions between Tin Oxide Nanoparticles and Electrostatically-Bound Molecular Reactants. *J. Am. Chem. Soc.* **2000**, *122*, 10956−10963.
(15) Gerischer, H.; Willig, F. Reaction of Excited Dye Molecules at Electrodes. *Top. Curr. Chem.* **1976**, *61*, 31−84.
(16) Marcus, R. A. Chemical and Electrochemical Electron-Transfer Theory. *Annu. Rev. Phys. Chem.* **1964**, *15*, 155−196.
(17) Kuciauskas, D.; Freund, M. S.; Gray, H. B.; Winkler, J. R.; Lewis, N. S. Electron Transfer Dynamics in Nanocrystalline Titanium Dioxide Solar Cells Sensitized with Ruthenium or Osmium Polypyridyl Complexes. *J. Phys. Chem. B* **2001**, *105*, 392−403.
(18) Ramakrishna, G.; Ghosh, H. N.; Singh, A. K.; Palit, D. K.; Mittal, J. P. Dynamics of Back-Electron Transfer Processes of Strongly Coupled Triphenyl Methane Dyes Adsorbed on TiO_2 Nanoparticle Surface as Studied by Fast and Ultrafast Visible Spectroscopy. *J. Phys. Chem. B* **2001**, *105*, 12786−12796.
(19) Brennaman, M. K.; Patrocinio, A. O. T.; Song, W.; Jurss, J. W.; Concepcion, J. J.; Hoertz, P. G.; Traub, M. C.; Murakami Iha, N. Y.; Meyer, T. J. Interfacial Electron Transfer Dynamics Following Laser Flash Photolysis of $[Ru(bpy)_2((4,4'\text{-}PO_3H_2)_2bpy)]^{2+}$ in TiO_2 Nanoparticle Films in Aqueous Environments. *ChemSusChem* **2011**, *4*, 216−227.

DOI: 10.1021/acs.jpcc.5b03477
J. Phys. Chem. C 2015, 119, 14929−14937

(20) Yan, S. G.; Prieskorn, J. S.; Kim, Y.; Hupp, J. T. In Search of the Inverted Region: Chromophore-Based Driving Force Dependence of Interfacial Electron Transfer Reactivity at the Nanocrystalline Titanium Dioxide Semiconductor/Solution Interface. *J. Phys. Chem. B* **2000**, *104*, 10871−10877.
(21) Schlichthörl, G.; Huang, S. Y.; Sprague, J.; Franck, A. J. Band Edge Movement and Recombination Kinetics in Dye-Sensitized Nanocrystalline TiO_2 Solar Cells: A Study by Intensity Modulated Photovoltage Spectroscopy. *J. Phys. Chem. B* **1997**, *101*, 8141−8155.
(22) Salvador, P.; Hidalgo, M. G.; Zaban, A.; Bisquert, J. Illumination Intensity Dependence of the Photovoltage in Nanostructured TiO_2 Dye-Sensitized Solar Cells. *J. Phys. Chem. B* **2005**, *109*, 15915−15926.
(23) Ondersma, J. W.; Hamann, T. W. Recombination and Redox Couples in Dye-Sensitized Solar Cells. *Coord. Chem. Rev.* **2013**, *257*, 1533−1543.
(24) Bisquert, J.; Zaban, A.; Salvador, P. Analysis of the Mechanisms of Electron Recombination in Nanoporous TiO_2 Dye-Sensitized Solar Cells. Nonequilibrium Steady-State Statistics and Interfacial Electron Transfer via Surface States. *J. Phys. Chem. B* **2002**, *106*, 8774−8782.
(25) Bisquert, J.; Zaban, A.; Greenshtein, M.; Mora-Sero, I. Determination of Rate Constants for Charge Transfer and the Distribution of Semiconductor and Electrolyte Electronic Energy Levels in Dye-Sensitized Solar Cells by Open-Circuit Photovoltage Decay Method. *J. Am. Chem. Soc.* **2004**, *126*, 13550−13559.
(26) Martinson, A. B. F.; Hamann, T. W.; Hupp, J. T. New Architectures for Dye-Sensitized Solar Cells. *Chem.—Eur. J.* **2008**, *14*, 4458−4467.
(27) Nelson, J. Continuous-Time Random-Walk Model of Electron Transport in Nanocrystalline TiO_2 Electrodes. *Phys. Rev. B* **1999**, *59*, 15374−15380.
(28) Nelson, J.; Chandler, R. Random Walk Models of Charge Transfer and Transport in Dye Sensitized Systems. *Coord. Chem. Rev.* **2004**, *248*, 1181−1194.
(29) Katoh, R.; Furube, A.; Barzykin, A. V.; Arakawa, H.; Tachiya, M. Kinetics and Mechanism of Electron Injection and Charge Recombination in Dye-Sensitized Nanocrystalline Semiconductors. *Coord. Chem. Rev.* **2004**, *248*, 1195−1213.
(30) Renault, C.; Nicole, L.; Sanchez, C.; Costentin, C.; Balland, V.; Limoges, B. Unraveling the Charge Transfer/Electron Transport in Mesoporous Semiconductive TiO_2 Films by Voltabsorptometry. *Phys. Chem. Chem. Phys.* **2015**, *17*, 10592−10607.
(31) Sakanati, Y.; Grosso, D.; Nicole, L.; Boissière, C.; Soler-Illia, G. J.; de, A. A.; Sanchez, C. Optimised Photocatalytic Activity of Grid-Like Mesoporous TiO_2 Films: Effect of Crystallinity, Pore Size Distribution, and Pore Accessibility. *J. Mater. Chem.* **2006**, *16*, 77−82.
(32) Bard. A. J.; Faulkner, L. R. *Electrochemical Methods: Fundamentals and Applications,* 2nd ed.; Wiley: New York, 2001.
(33) This conclusion is actually obtained on the basis of a simple model assuming a constant apparent diffusion coefficient of electrons. This assumption is rough because electron diffusion probably occurs through a trapping-detrapping process of electrons from deep trap states to conduction band, and the electron occupancy in these traps is potential-dependent, thus resulting in a potential dependent diffusion coefficient. We can here simply propose that $l_e = (d_f/(D_e RT/Fv)^{1/2}) \ll 1$ at any potential.
(34) Boschloo, G.; Fitzmaurice, D. Spectroelectrochemical Investigation of Surface States in Nanostructured TiO_2 Electrodes. *J. Phys. Chem. B* **1999**, *103*, 2228−2231.
(35) That such a simplification holds in the present experimentally studied system has been proved by analysis of cyclic voltammograms on the very same films in the absence of redox probe (see Figure 6 in reference 30).
(36) Bisquert, J. Physical Electrochemistry of Nanostructured Devices. *Phys. Chem. Chem. Phys.* **2008**, *10*, 49−72.
(37) Agrell, H. G.; Boschloo, G.; Hagfeldt, A. Conductivity Studies of Nanostructured TiO_2 Films Permeated with Electrolyte. *J. Phys. Chem. B* **2004**, *108*, 12388−612396.
(38) Fisher, A. C.; Peter, L. M.; Ponomorev, E. A.; Walker, A. B.; Wijayantha, K. G. U. Intensity Dependence of the Back Reaction and Transport of Electrons in Dye-Sensitized Nanocrystalline TiO_2 Solar Cells. *J. Phys. Chem. B* **2000**, *104*, 949−958.
(39) Clifford, J. D.; Palomares, E.; Nazeeruddin, Md. K.; Grätzel, M.; Nelson, J.; Li, X.; Long, N. J.; Durrant, J. R. Molecular Control of Recombination Dynamics in Dye-Sensitized Nanocrystalline TiO_2 Films: Free Energy vs Distance Dependence. *J. Am. Chem. Soc.* **2004**, *126*, 5225−5233.
(40) Clifford, J. D.; Yahioglu, G.; Milgrom, L. R.; Durrant, J. R. Molecular Control of Recombination Dynamics in Dye Sensitised Nanocrystalline TiO_2 Films. *Chem. Commun.* **2002**, 1260−1261.
(41) Chen, W.-C.; Marcus, R. A. Theory of a Single Dye Molecule Blinking with a Diffusion-Based Power Law Distribution. *J. Phys. Chem. C* **2012**, *116*, 15782−15789.

DOI: 10.1021/acs.jpcc.5b03477
J. Phys. Chem. C 2015, 119, 14929−14937